

1. Cosmology and Dark Matter Halos

1.1. The Cosmological Model

The concordance cosmological model, cold dark matter, has had great success in reproducing the CMB and predicting the behavior of radiation and baryons prior to the time when interactions (collisions) of the baryons and of the dark matter became important. The high density of the early Universe guarantees interactions at rates faster than the expansion, hence equilibrium between the various components. When a specific rate for collisions or some other type of interaction of particles and/or photons becomes smaller than the expansion rate $H(t)$, at that time the reaction falls out of equilibrium.

The physics of the evolution of the dark matter is straightforward and there are no parameters (aside from things like the number of neutrino flavors) with unknown values. Until collisions of particles become important, the properties of a Universe with collisionless cold dark matter and radiation can be solved analytically.

The general relativity metric for a spatially homogeneous and isotropic universe (the Friedman-Robertson-Walker metric) can be written as:

$$ds^2 = dt^2 - a^2(t) \left[\frac{dR^2}{1 - kR^2} + R^2(d\theta^2 + \sin^2\theta d\phi^2) \right],$$

where $a(t)$ is the cosmic scale factor which describes the expansion with time and k is the curvature parameter determining the geometry of the metric (what happens at large distance to a pair of freely traveling particles initially moving on parallel trajectories); $k > 0$ in a closed Universe, 0 in a flat Universe, and negative in an open Universe.

Light emitted at a time t is observed at the present ($t = 0$) with a redshift $z = [1/a(t)] - 1$, where a at the present time is defined to be 1.0, so that $a(t) < 1$ in the

past. (Sometimes $t = 0$ is set to the moment of the Big Bang, which may cause confusion.)

The Hubble constant is

$$H = \frac{da/dt}{a}.$$

By definition, its value at times near the present is da/dt . From the Friedman equation in general relativity, we find $H^2(t) = (8\pi G/3)\rho - k/a^2$.

The critical density required for a flat Universe (one with $k = 0$) is $\rho_c(t) = 3H^2(t)/(8\pi G)$, which is $\approx 9 \times 10^{-30}$ g/cm³ today. The ratio of the total density to the critical density is called Ω . There are contributions to Ω from matter (including baryons as well as dark matter) and from radiation. If we consider times close to the present, where radiation plays a minor role, and set $\Omega_k \equiv -(k/H_0^2) = 1 - \Omega_m$, then the Einstein-de Sitter model (which is a flat universe with $k = 0$ defined by $\Omega_m = 1$, $\Omega_\Lambda = \Omega_r = \Omega_k = 0$, where Ω_Λ is the term from the vacuum density (i.e. the cosmological constant) has the solution $a(t) \propto t^{2/3}$. However, if radiation dominates, then $a \propto t^{1/2}$

For the flat Einstein-de Sitter model described above with $a(t) \propto t^{2/3}$, $H(t) = (2/3)t^{-1}$. The Hubble constant today is denoted by H_0 ; its current value is set to $h \times 100$ km/sec/Mpc to encompass the range of values of H_0 established from observations of the velocity of recession of galaxies in the past three decades. Recent measurements of h are all near 0.70; see the papers from the Hubble Treasury program on Cepheid variables in nearby galaxies, e.g. Freedman, Madore, Gibson et al. (2001, ApJ, 553, 47) and references therein. Then $H_0 t_0 = 2/3$, where t_0 is the age of the Universe. The age of the universe in this model is $1/H_0 \equiv (10^{10}/h)$ yr = $(10/h)$ Gyr. Stellar astrophysics demands a t_0 of order 12 Gyr.

One can show that at high redshift (i.e. when $1 + z \gg |\Omega_m - 1|$ assuming Ω_r can be neglected) models with non-zero Ω_k or Ω_Λ approach the Einstein-de Sitter solution.

In this regime the age of the Universe to a redshift z is

$$t \text{ from Big Bang} \approx \frac{2}{3H_0\sqrt{\Omega_m}}(1+z)^{-3/2}$$

In the standard hot Big Bang model, the energy density of the initially hot Universe is dominated by radiation. The energy a non-relativistic particle is fixed and is mc^2 . The energy density of such particles is proportional to $1/\text{Volume}$, hence $a(t)^{-3}$. The energy of a photon is proportional to λ^{-1} . Thus the photon temperature is $T(t) = T_0/a(t)$, where $T_0 = 2.63$ K is the temperature of the relic Big Bang radiation at the present time, which radiation we call the CMB (cosmic microwave background). The volume energy density of the photons is proportional to $a(t)^{-4}$.

Since $a(t)^{-4}$ declines more rapidly than $a(t)^{-3}$ as a increases and one approaches the present time, eventually a transition from radiation domination to matter domination must occur. This happens at a_{eq} , for which $z \sim 3500$, when the universe was $\approx 65,000$ yr old. The gas at that point is still ionized, and the matter and radiation are still coupled.

At $z \sim 1100$ (age $\sim 300,000$ yr) the temperature drops below 3000 K, and recombination of the protons and electrons to form neutral H atoms occurs. This is a thermal energy well below 13.6 eV, the ionization potential of H, but the high photon/baryon ratio ensures that as soon as a neutral H is produced it will be instantaneously ionized. Reionization does not occur until $T_K \sim 1$ eV. Once neutral H atoms exist as a substantial fraction of the baryons, the Universe became transparent to photons. The photons decoupled from the gas, and the relic Big Bang photons from that time on travel freely, cooling with time. These are the CMB photons we observe today, which currently have $T = 2.63$ K with a uniformity in T of this blackbody radiation field of better than 0.1% over the sky.

The currently accepted concordance cosmology has parameters $\Omega_m = 0.24$, $\Omega_b =$

0.04, $\Omega_\Lambda = 0.73$. It satisfactorily explains the Hubble diagram for galaxies indicating expansion, the abundances of the lightest elements via Big Bang nucleosynthesis, and the existence and properties of the CMB. However, all of the galaxies and stars and gas we have studied for years are only 4% of the total. We do not know anything about the nature of dark matter, and even less about “dark energy” (i.e. Ω_Λ). This is a very unsatisfactory and frustrating state of affairs.

The cosmological parameter w , determined by the 5 year results from WMAP (a satellite that measured the CMB very accurately) to be -0.99 ± 0.06 and sought to still higher precision from many more planned experiments, is related to the equation of state of the “dark energy” (the cosmological constant). For matter, $w = 0$, for a cosmological constant, $w = -1$.

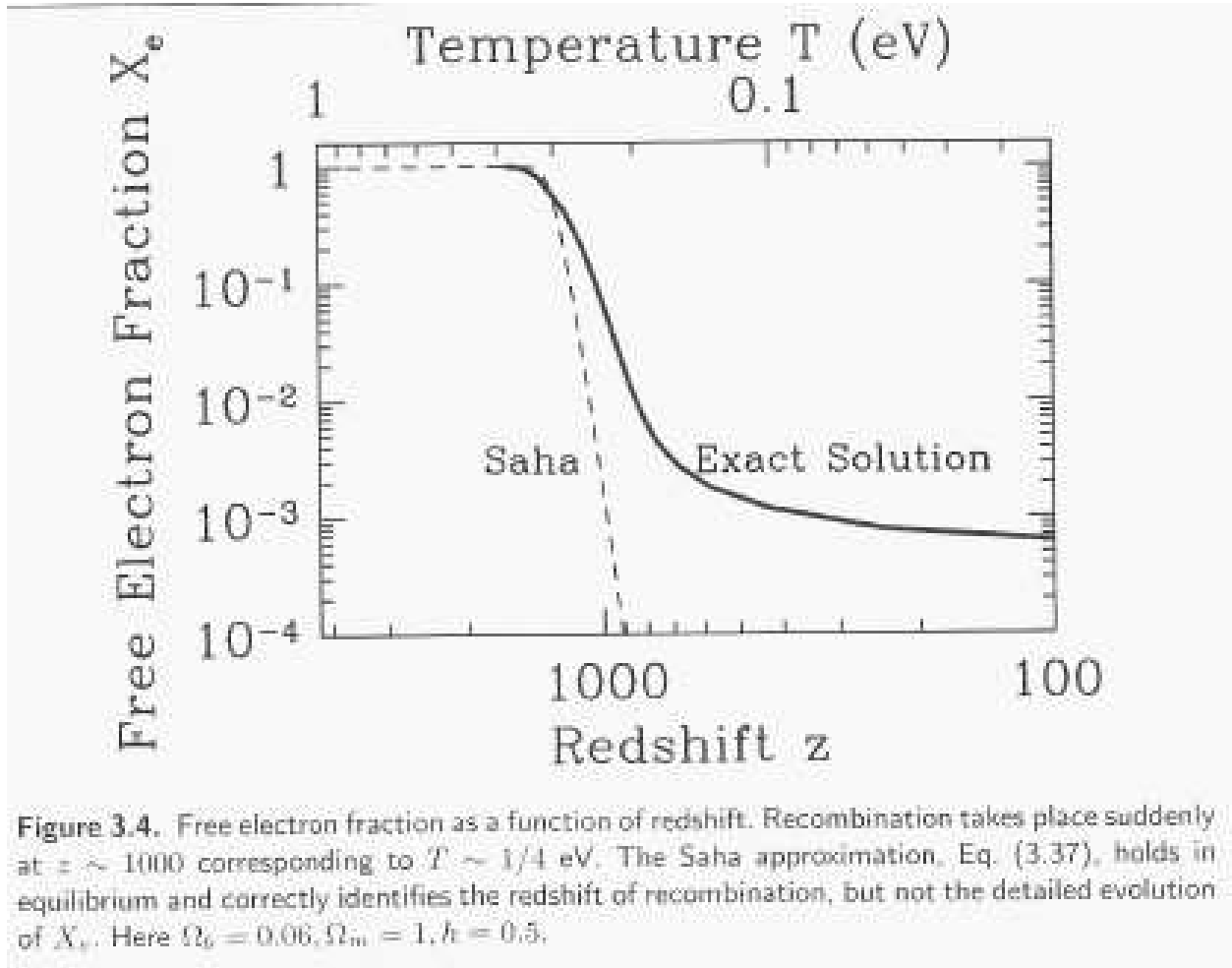


Fig. 1.— Fig. 3-4 from Dodelson, *Modern Cosmology*.

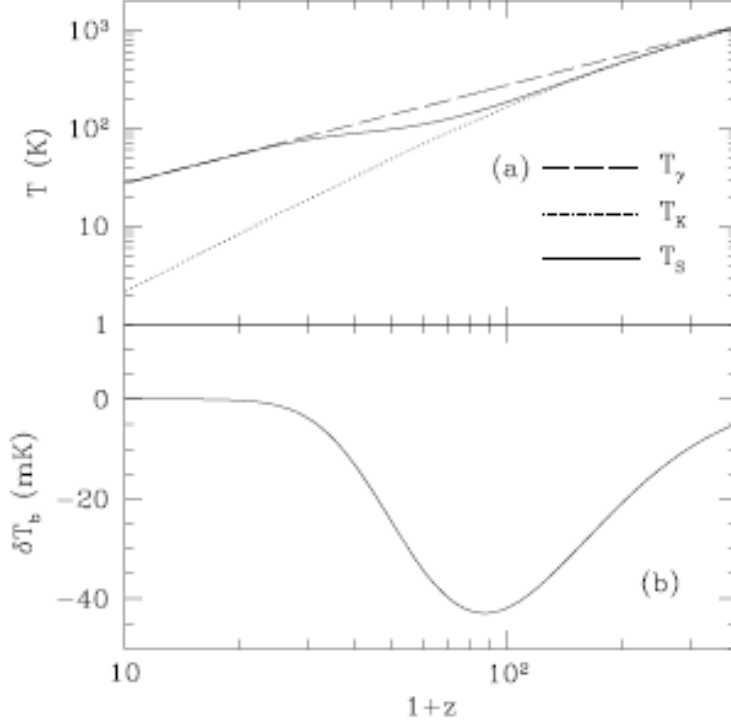


Fig. 6. (a): IGM temperature evolution if only adiabatic cooling and Compton heating are involved. The spin temperature T_S includes only collisional coupling. (b): Differential brightness temperature against the CMB for T_S shown in panel a.

Fig. 2.— IGM temperature evolution ignoring star formation and stellar energy input into the IGM. In the upper panel, the straight dashed line is the photon temperature, the solid line just below it and sometimes overlapping is the spin temperature for excitation within the ground state of HI (the 21 cm line transition), and the dotted line dropping rapidly towards low z is the dark matter kinetic temperature. The lower panel is the differential brightness temperature of T_S , the hydrogen spin temperature, which determines the strength of the (reshifted) 21 cm line, against the CMB. (Fig. 6 from Furlanetto, Peng Oh & Briggs, 2006, Phys. Reports, 433, 181, a lengthy review *Cosmology at Low Frequencies: The 21 cm Transition and the High Redshift Universe*.)

1.2. Primordial Fluctuations

Primordial fluctuations in the density field were generated by quantum mechanical fluctuations at the end of the epoch of inflation. Inflation stretched a region of microscopic size to a scale bigger than the visible Universe and thus our local geometry became flat. Inflation solves the “horizon problem”.

The horizon problem arises as the event horizon in a decelerating universe scales as a^b , with $b > 0$. For a matter dominated universe, this is $a^{1/2}$. The CMB decoupled at $a = 10^{-3}$, so the horizon at that time subtended an angle on the sky of $10^{-3/2}$ radians, or ≈ 2 deg. This means there were at that time $\sim 10^4$ causally disconnected regions, yet we know that the CMB sky today is isotropic in temperature to better than 1 part in 10^5 .

At the epoch of the emission of the CMB, the fluctuations in the energy density and gravitational potential were about 1 part in 10^5 . Measuring this with some degree of precision is one of the observational triumphs of the past decade. Let $\delta(x) = (\rho(r)/\langle \rho \rangle) - 1$, where $x = r/a(t)$ is a comoving position and r is the associated physical coordinate. Recall that for 2 points, the comoving distance is fixed as the universe expands, while the physical distance expands with $a(t)$ such that the Hubble flow velocity $\mathbf{v} = d\mathbf{r}/dt = H(t) \mathbf{r}$, where boldface denotes vectors.

Since the universe is homogenous on large scales, $\delta \ll 1$ on large scales

The potential ϕ is from Poisson’s equation, $\delta^2\phi = 4\pi G \langle \rho \rangle a^2\delta$, and this equation describes the evolution of collisionless CDM particles. The equation of continuity and Euler’s equation (a force balance) describe the motions. The first of these, for \mathbf{u} being the peculiar velocity with respect to the Hubble flow, $\mathbf{u} = \mathbf{v} - H\mathbf{r}$, is

$$\frac{\partial\delta}{\partial t} + \frac{1}{a} \nabla \cdot [(1 + \delta)\mathbf{u}] = 0,$$

These two equations, combined with Poisson’s equation, and linearized for small perturbations, give an expression for the growth of perturbations with time,

$$\frac{\partial^2 \delta}{\partial t^2} + 2H \frac{\partial \delta}{\partial t} = 4\pi G \langle \rho \rangle \delta.$$

This equation has a growing and decaying solution, of which only the growing mode is important after a short time. Thus, until it becomes non-linear, the density perturbation has a fixed shape and grows in amplitude by a factor which depends on time. For the Einstein-de Sitter model, this growth factor is proportional to $a(t)$.

We now need to look at the spatial form of the density fluctuations. There is no coupling in the equations above between different harmonic components. Thus each mode is independent. Inflation generates fluctuations which can be described by a Gaussian random field, so that the different k -modes (where $k = 2\pi/\lambda$) are statistically independent. It is believed that inflation generates a power spectrum of fluctuations $P(k) \propto k^n$ with $n \approx 1$. The modified power spectrum in the Universe at late times has a turnover at a scale cH^{-1} at matter-radiation equality, and a small scale asymptotic shape $P(k) \propto k^{n-4}$.

The two point correlation function (the autocorrelation function of the density field) is $\xi(\mathbf{r}) = \langle \delta(\mathbf{x})\delta(\mathbf{x} + \mathbf{r}) \rangle$. This can be measured through the clustering of objects (halos or galaxies). The power spectrum is the Fourier transform of the two point correlation function. It is much harder to determine from observations, but is much easier to predict from the theory.

To consider the fluctuations which might give rise to a mass M , we consider a spherical top hat, smoothing the density perturbation field over a sphere of radius R and ignoring anything outside that region. The normalization of the density fluctuations, which can’t be derived from first principles, is usually specified by the value $\sigma_8 \equiv \sigma(R = 8h^{-1} \text{ Mpc})$,

which is observed to be ~ 1 at the present epoch. Here σ is the rms deviation of the density field smoothed by a window function normalized to unity.

For the top-hat window function, the smoothed perturbation field is denoted by δ_R or δ_M , where $M = 4\pi\rho_m R^3/3$, and ρ_m is the current mean density of matter and R is the comoving radius. The variance $\langle \delta_M \rangle^2$, denoted $\sigma^2(M)$, is an important parameter in estimates of the abundance of collapsed objects as a function of time.

The decoupling of (dark) matter from the radiation affects the perturbation fluctuations. The interaction cross section of the dark matter particles sets the epoch at which decoupling occurs. There is both thermal decoupling (the temperature of the matter and photons is no longer identical) and kinematic decoupling (the bulk motion of the two starts to differ). These occur at the same epoch for CDM, when the timescale for collisions to change the momentum of the particles becomes equal to the Hubble time. The particle mass determines the spread of thermal speeds of the particles, which smoothes out very small scale fluctuations after kinematic decoupling. Viscosity also smoothes fluctuations in the particle density. Also we need to consider the effect of the acoustic oscillations of the radiation (i.e. the fluctuations in the CMB radiation field) on the particle density fluctuations at decoupling.

Note that the CDM damping scale is significantly smaller than the scales directly observed in the CMB photons due to the viscosity of the CDM particles. A smaller value of k is equivalent to a larger value of R in computing the minimum mass of dark matter clumps. The result of a detailed analysis of these effects (see A. Loeb’s chapter in *First Light*) is that acoustic oscillations truncate the CDM power spectrum on a comoving scale even larger (i.e. a k even smaller) than other effects listed above. This increases the minimum mass of dark matter clumps by more than a factor of 10 to a value $M = 4\pi\rho_c\Omega_M(\pi/k_{cut})^3/3 \approx 10^{-4}(T_d/10 \text{ MeV})^{-3}M_\odot$. Here k_{cut} is the wave number where

the transfer function for the fluctuations drops to a fraction $1/e$ of its value as $k \rightarrow 0$, $k_{cut} \approx 3.3\eta_d^{-1}$, where η_d is the free streaming damping scale, so the scale length ratio differs by $\approx 3.3^3$.

We now consider the early evolution of perturbations of the baryons. They are coupled to the radiation field by Thomson scattering until the baryons become neutral. After cosmic recombination, they start to fall into the potential wells of the dark matter. Since the baryons are a small fraction of the total matter, we do not consider this issue in detail.

Initially all modes are outside the horizon and the gravitational potential is constant. At intermediate times, the wavelengths fall within the horizon and the universe evolves from radiation domination to matter domination. Large scale modes, which enter the horizon after the universe becomes matter dominated, evolve differently than small scale modes. At late times, all the modes evolve identically again.

Structures (galaxies, dark matter halos) will form around the highest density perturbations. Observations suggest that galaxies (i.e. matter) have a higher two point correlation function than does dark matter. Some people introduce biasing to try to reproduce this, introducing a bias factor b , $b > 1$, such that $(\delta\rho/\rho)(\text{for galaxies}) = b(\delta\rho/\rho)$ for dark matter. This ensures that galaxies (matter) collapse only around even higher density perturbations than does the dark matter.

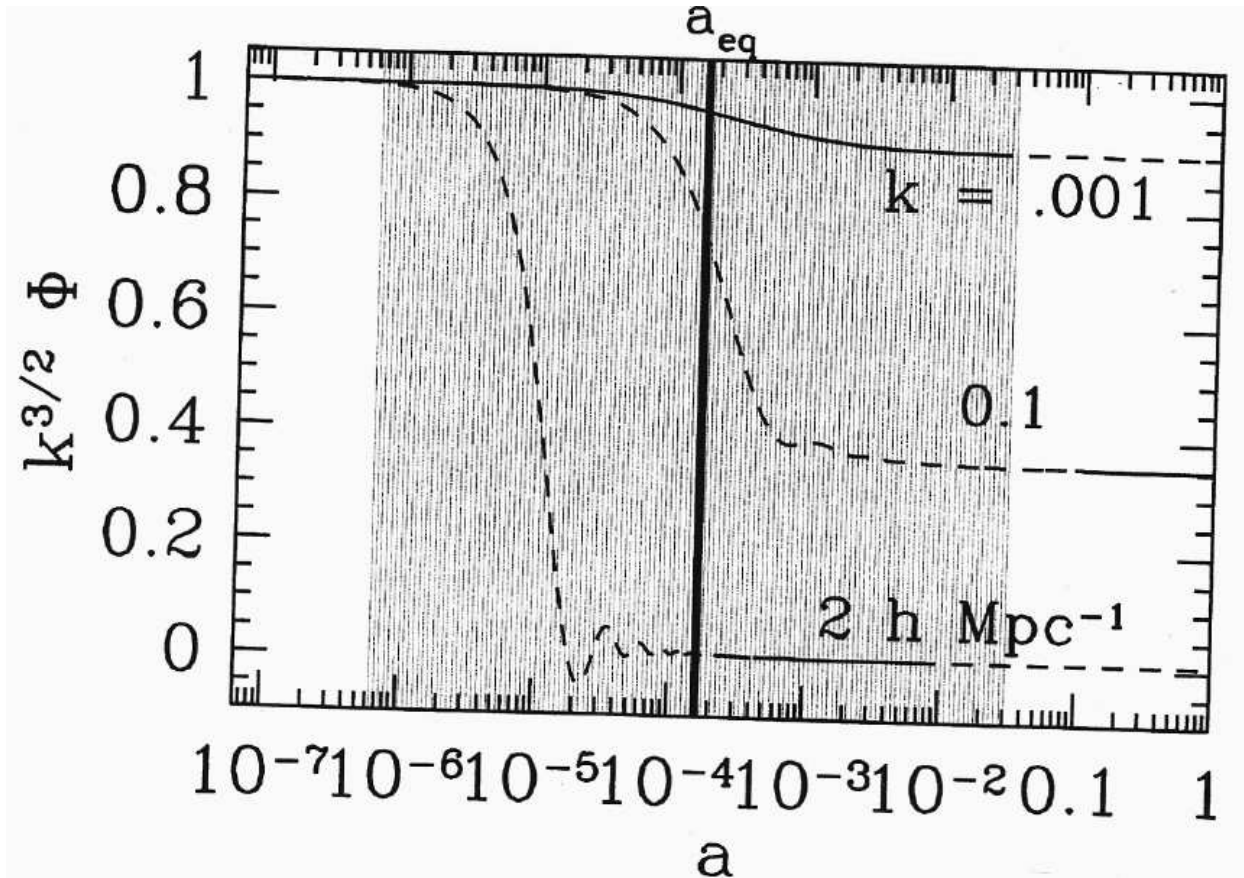


Fig. 3.— The linear evolution of the gravitational potential ϕ . A dashed line denotes that the mode has entered the horizon. The thick vertical line denotes the time when the universe transitions from being radiation dominated to matter dominated. Evolution through the shaded region is described by the transfer function. The potentials are all set to 1 at very high redshift. The relative normalization of the three modes is as it would be for scale-invariant perturbations. Baryons have been neglected, $\Omega_m = 1$, and $h = 0.5$. (Fig. 7-2 from Dodelson, *Modern Cosmology*).

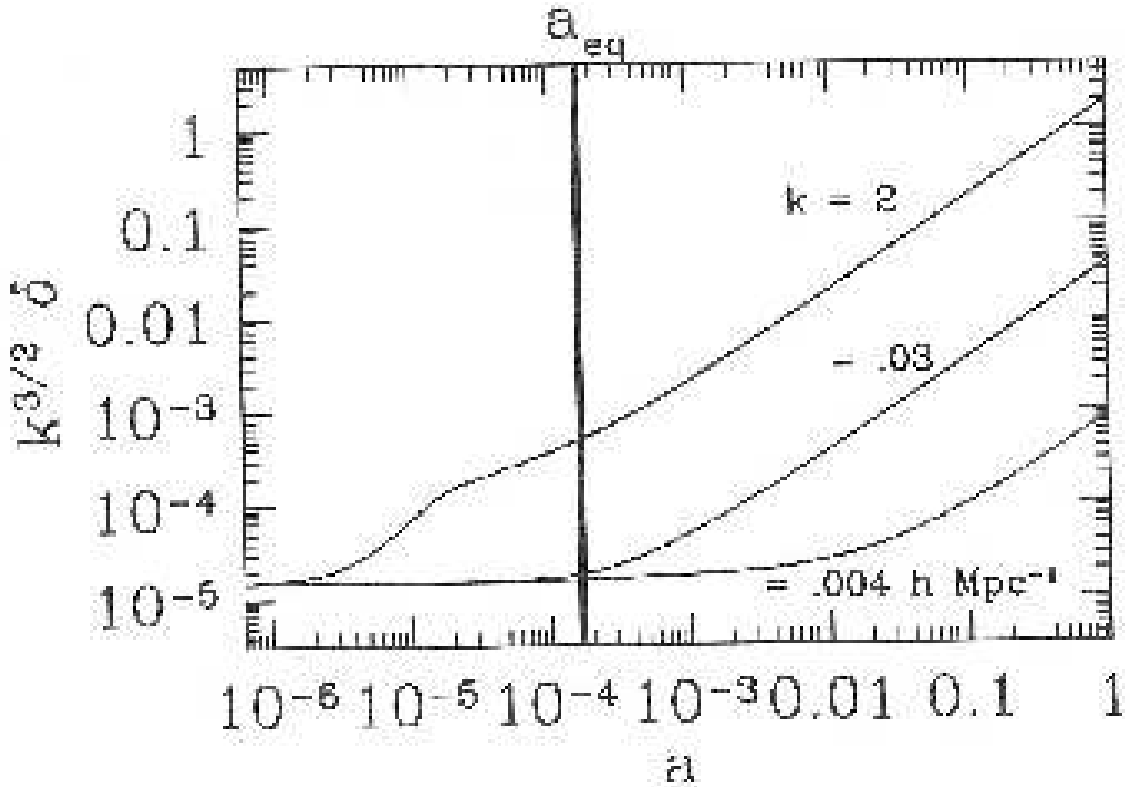


Fig. 4.— (Dodelson, fig. 7-3) The evolution of perturbations to the dark matter in the same model as used for Fig. 7-2. Amplitude starts to grow upon horizon entry (different times for the three different modes shown). Well after a_{eq} (a when the matter and radiation energy densities are equal), all sub-horizon modes evolve identically, scaling as the growth factor. In the case plotted, a matter dominated flat universe (Einstein-de Sitter case), the growth factor is equal to $a(t)$.

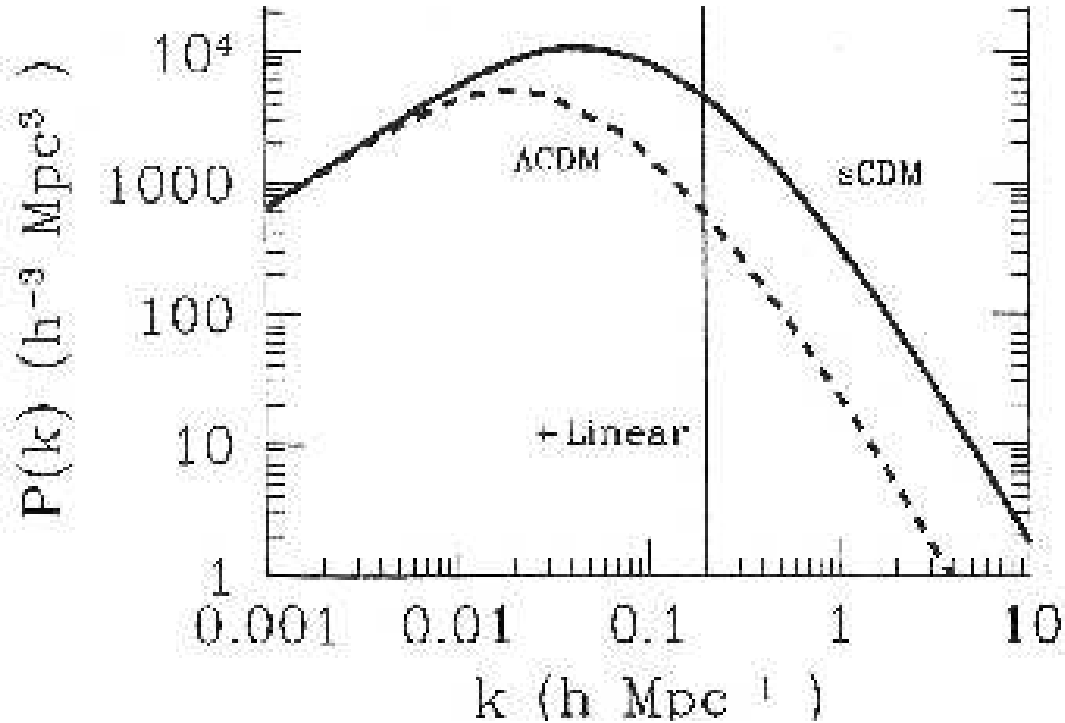


Fig. 5.— The power spectrum in two CDM models, with dark energy and without a cosmological constant. The units of the horizontal axis are $k(h \text{ Mpc}^{-1})$. The spectra have been normalized to agree on large spatial scales (small k). The spectrum with dark energy turns over at larger scales because of a later transition from radiation to matter domination. Scales to the left of the vertical line are still evolving linearly. The turnover occurs at a scale corresponding to the one which enters the horizon just as the universe switches from being radiation to matter dominated. The decline at small scale lengths (large k) occurs because of the decline of the transfer function of a mode during the radiation epoch. The scale over which the linear case is valid ends when $\Delta(k_{nl}) = 1$. (Fig. 7-4 from Dodelson, *Modern Cosmology*).

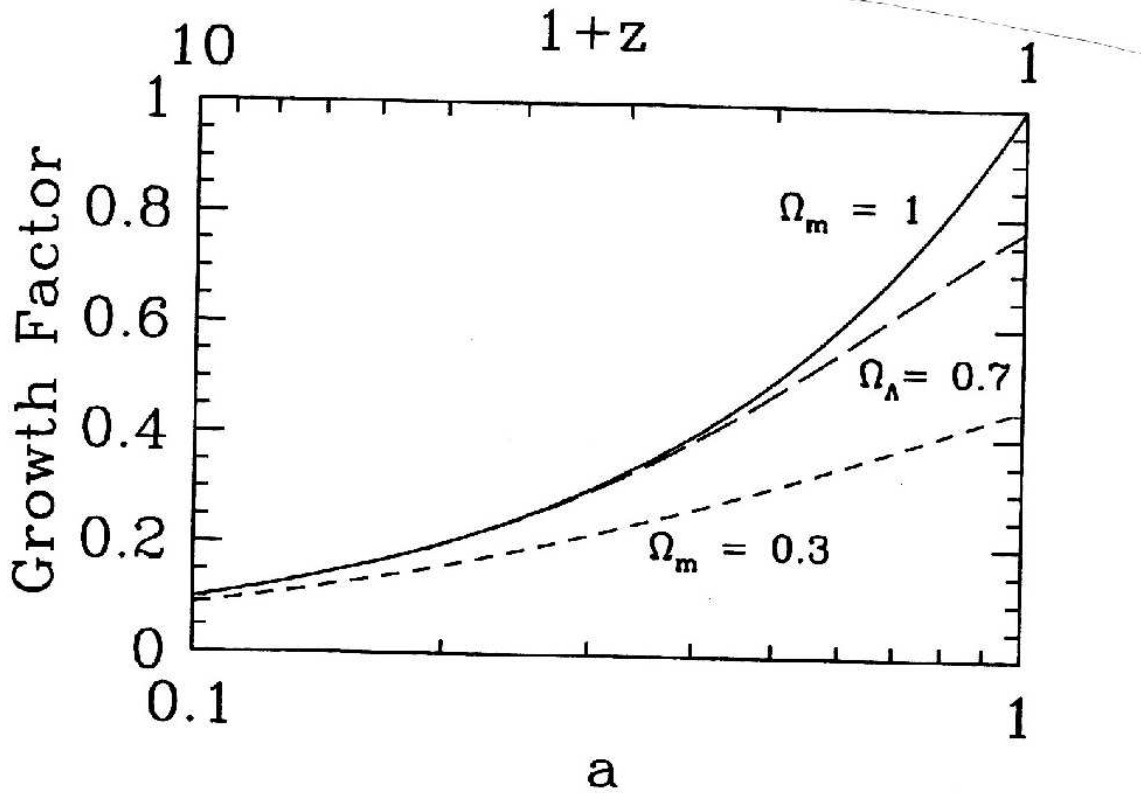


Figure 7.12. The growth factor in three cosmologies. Top two curves are for flat universes without and with a cosmological constant. Bottom curve is for an open universe.

Fig. 6.— The growth factor at late times, $z < 10$, for three different cosmologies. For a flat matter dominated universe, the growth factor is equal to the scale factor, $a(t)$. The growth factor is lower at late times in open and dark energy cosmologies than in the $\Omega_m = 1$ cosmology, indicating that the large scale structure we observe today had to form earlier in such models. This affects the prediction for the number of galaxy clusters as a function of z , etc. Fig. 7-12 from Dodelson, *Modern Cosmology*.

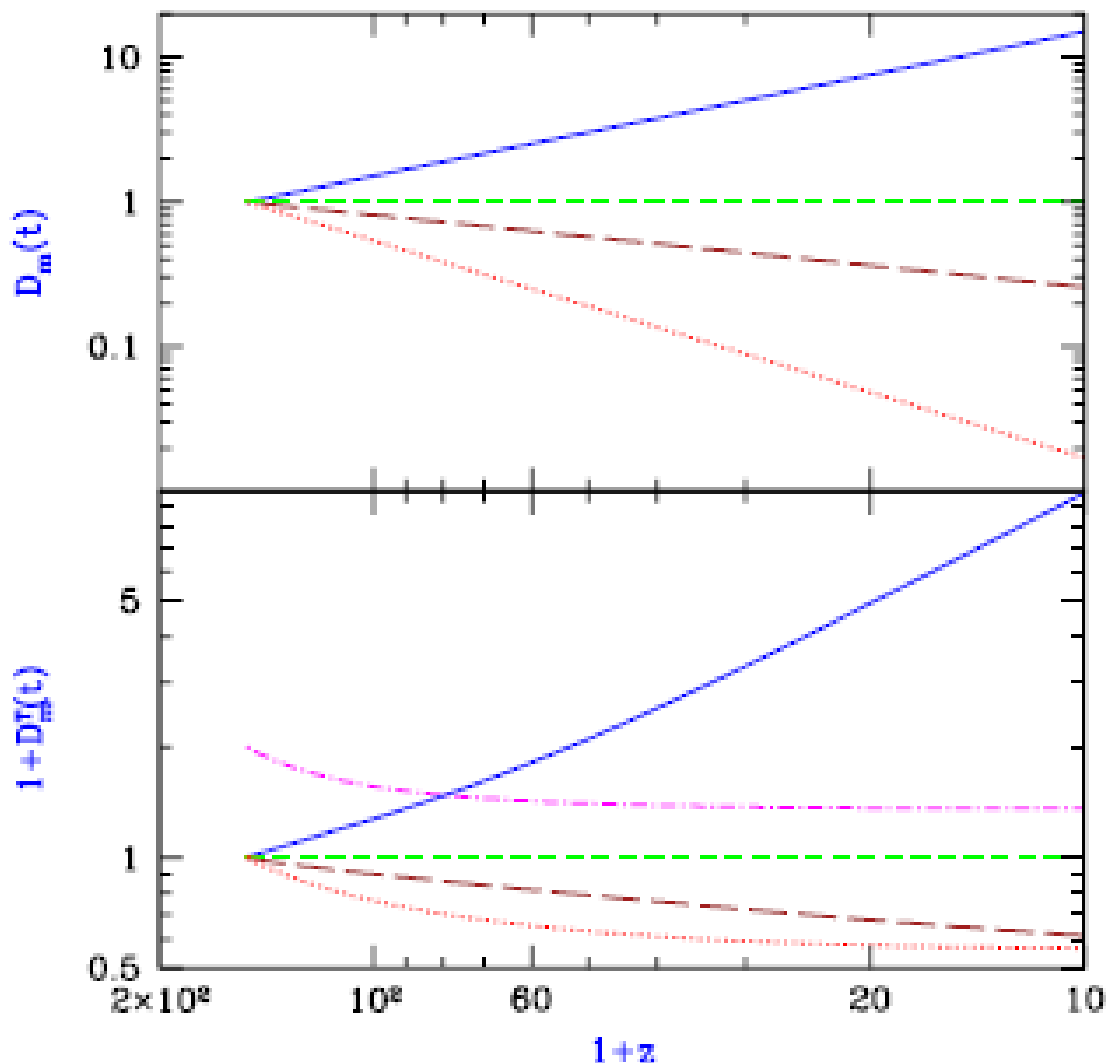


Figure 1. Redshift evolution of the amplitudes of the independent modes of the density perturbations (upper panel) and the temperature perturbations (lower panel), starting at redshift 150. We show $m = 1$ (solid curves), $m = 2$ (short-dashed curves), $m = 3$ (long-dashed curves), $m = 4$ (dotted curves), and $m = 0$ (dot-dashed curve). Note that the lower panel shows one plus the mode amplitude.

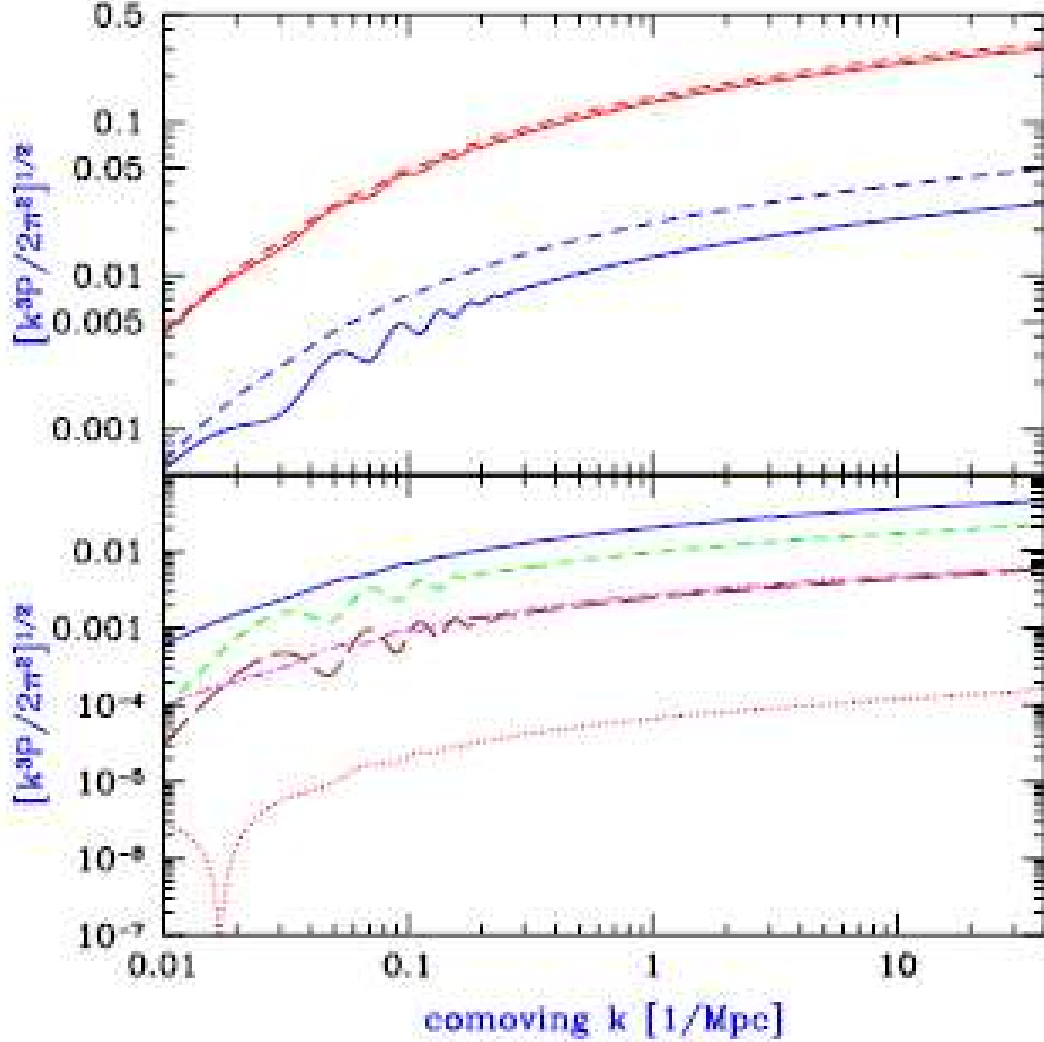


Figure 2. Power spectra and initial perturbation amplitudes versus wavenumber. The upper panel shows $\bar{\delta}_b$ (solid curves) and $\bar{\delta}_{\text{dm}}$ (dashed curves) at $z = 150$ and 20 (from bottom to top). The lower panel shows the initial ($z = 150$) amplitudes of $\bar{\delta}_1$ (solid curve), $\bar{\delta}_2$ (short-dashed curve), $\bar{\delta}_3$ (long-dashed curve), $\bar{\delta}_4$ (dotted curve), and $\bar{\delta}_T(t_i)$ (dot-dashed curve). Note that if $\bar{\delta}_1$ is positive then so are $\bar{\delta}_3$ and $\bar{\delta}_T(t_i)$, while $\bar{\delta}_2$ is negative at all k , and $\bar{\delta}_4$ is negative at the lowest k but is positive at $k > 0.017 \text{ Mpc}^{-1}$.

1.3. Gravitational Instability

A summary of the discussion of the growth of perturbations in the dark matter given above is that before the mode enters the horizon, everything is coupled and nothing happens. Evolution thereafter is described by a transfer function which strongly suppresses modes that enter the horizon before the transition from radiation dominance to matter dominance, while those modes with large enough scale (k small enough) that they do not enter the horizon until this transition has already occurred are only slightly suppressed. At late times, all the modes evolve identically again, irrespective of their spatial scale k .

The force on an element near an overdensity of matter ($\delta\rho_m > 1$) is determined by the difference between the pressure and the gravitational forces. If the pressure is high, then random thermal motions cause a diffusion of particles out of an overdense region. Inhomogeneities cannot grow, and $\delta\rho$ will oscillate with time. If the pressure is low, then an overdensity can grow exponentially.

This is parameterized by the Jeans length which in Newtonian gravity defines the critical λ separating the oscillatory and exponential solutions for growth of perturbations in an infinite, uniform, and stationary gas distribution. For scales smaller than λ_J , the sound crossing time l/c_s is shorter than the gravitational free fall time ($\propto G\rho$)^{-1/2} allowing the build up of a pressure force that can counteract gravity. On larger scales, the pressure builds up too slowly to react to the building up of the attractive gravitational force, and collapse follows.

The Jeans mass is that within a spherical volume of radius $\lambda_J/2$. This is the minimum mass that can collapse under the given conditions. This mass can be derived by considering the borderline case when the cloud of mass M and radius R is in hydrostatic equilibrium by replacing dP/dr by $-P/R$ and assuming an ideal gas to get $M_J \sim [kT/(m_p G)]^{3/2} \rho^{-1/2}$. This, evaluated for cold cloud cores in the Solar neighborhood with $T \sim 10$ K, yields a value

of $\sim 0.5M_\odot$. But the value of M_J in the early Universe is much larger due to the higher T and lower ρ .

For cosmological purposes, we need a Jeans mass calculation that considers a single Fourier mode with a spherical spatial fluctuation on scales much smaller than the horizon, includes dark matter and baryons, and includes expansion of the Universe.

T of the baryons follows that of the CMB photons until decoupling; in this regime $T_b \propto (1+z)$. After the residual electrons (fraction of ionized H) declines sufficiently so that all coupling with the photons is lost, the baryons expand adiabatically with the Universe, so $T \propto (1+z)^2$. In the adiabatic limit, T and ρ are related by $T_b \propto \rho_b^{\gamma-1}$, where γ is the adiabatic index of the baryon gas. Note that the mean atomic weight per particle in the gas μ for the neutral primordial gas is fixed, and is set by the Big Bang production of He to be 1.22.

The equation for the growth of baryon fluctuations including all the above factors again gives rise to a length scale which divides the oscillatory from the exponentially growing solutions, the cosmological Jeans length, which is time dependent. As time proceeds, perturbations with increasingly smaller initial wavelengths stop oscillating and start to grow.

In the regime from $z \sim 1100$ (the epoch of recombination) and the time z_t when there are no longer enough residual electrons to couple T_b to $T(CMB)$, we find $k_J \equiv (2\pi)/\lambda = [2kT_{CMB}/3\mu m_p]^{-1/2}\sqrt{\Omega_m}H_0$, so the Jeans mass (including both baryons and dark matter) is redshift independent and has the value $M_J = 1.4 \times 10^5 (\Omega_m h^2 / 0.15)^{-1/2} M_\odot$. The factor in parenthesis is ≈ 1 , so this is comparable to the mass of a globular cluster as observed today in the Milky Way halo.

At times later than z_t , the temperature of the matter declines adiabatically, and the total

Jeans mass becomes $M_J = 4.5 \times 10^3 (\Omega_m h^2 / 0.15)^{-1/2} (\Omega_b h^2 / 0.022)^{-3/5} [(1+z)/10]^{3/2} M_\odot$. This is $\sim 5,000 M_\odot$ at $z \sim 10$.

Another complication is that the Jeans mass is a function of time, but the linear theory applies only to the evolution of perturbations at a given time. Furthermore, as the perturbations grow, eventually δ reaches 1, and the linear perturbation treatment is no longer valid. After that time, the full non-linear gravitational problem must be solved.

The easiest case is spherical symmetry, with a top hat overdensity. We approximate this as a Newtonian case of a top hat with total mass $M = (4\pi/3)r_i^3 \rho_i (1 + \delta_i)$, where ρ_i is the initial background density and δ_i is the initial overdensity. Then the particle will either collapse, reach infinity with some positive velocity, or reach infinity with zero velocity. The latter defines the critical overdensity, which collapses to a point at $1 + z_c = 0.593\delta_i/a_i$. Thus a top hat sphere collapsing at redshift z_c had a linear overdensity extrapolated to the present time of $\delta_0 = 1.69(1 + z_c)$. In this case, a density perturbation at a redshift z with $\delta > 1.69/D(z)$, where $D(z) = (1+z)^{-1}$, will have collapsed to a point by the present time, with $\delta_{crit} = 1.69/D(z)$.

Numerical simulations of hierarchical halo interactions along these lines leads to a “universal” density profile for the resulting halos given by Navarro, Frenk & White (1997), which has the form

$$\rho(r) = \frac{3H_0^2}{8\pi G} (1+z)^3 \frac{\Omega_m}{\Omega_m^z} \frac{\delta_c}{c_N x (1 + c_N x)^2}$$

where $x = r/r_{vir}$. The characteristic density δ_c is a function of the concentration parameter c_N and of Δ_c , where Δ_c is the final overdensity relative to the critical density at the collapse radius, which is $18\pi^2 \approx 178$ in a Einstein-de Sitter universe.

$$\delta_c = \frac{\Delta_c}{3} \frac{c_N^3}{\ln(1 + c_N) - c_N/(1 + c_N)}$$

The virial temperature is that determined from the gravitational potential, so the kinetic energy for each particle, $(3kT/2)$, assumed to be protons, is the gravitational potential energy, $kT_{vir} = -(1/3)m_p\phi$, where ϕ is the gravitational potential. The virial radius refers to the radius of a sphere within which virial equilibrium holds. It is often assumed that this corresponds to the radius within which the average density is larger, by some specified factor, than the critical density for a flat universe $\rho_{crit} = (3H)^2/(8\pi G)$. The factor chosen must be big, usually 200 is the value adopted; the value 178 is the overdensity at virialization. Ignoring cosmology, one can follow a gas as it collapses, noting that when the radius is half the initial radius, if virial equilibrium holds, the gravitational potential is more negative by a factor of two, and the thermal energy is then $0.5 \times |\phi_i|$, where ϕ_i is the initial gravitational energy (assuming the initial thermal energy is very low). One can follow the collapse of dark matter perturbations in detail, and use the above to establish a specific criterion for virialization to have occurred.

There are some useful notes by Wayne Hu which work this out in detail (including the factor of 178), see http://background.uchicago.edu/~whu/Courses/Ast321_05/ast321_7.pdf, also A. Loeb's chapter in *First Light*, pages 30-36.

1.4. The Distribution of Dark Matter Halos with Mass

The number distribution of dark matter halos with mass at a redshift z is a key parameter in CDM theory. Press & Schechter (1974) worked this out, assuming a Gaussian random field of density perturbations, linear growth, and spherical collapse. The discussion begins with δ_M , the density field smoothed on a mass scale M , which is a function of

redshift, and has a mean of 0, with a standard deviation of $\sigma(M)$. One can then calculate the probability that δ_M is greater than some value δ by integrating the Gaussian distribution from δ to ∞ . This probability is taken as the fraction of dark matter particles which are in collapsed halos with mass greater than M . The result is the Press-Schechter function,

$$F(> M, z) = \text{erfc}[\delta_{\text{crit}}(z)/(\sqrt{2}\sigma(M))] = \frac{2}{\pi} \int_0^x e^{-t^2} dt$$

and $t = \delta_{\text{crit}}(z)/(\sqrt{2}\sigma(M))$.

Differentiating the above yields the mass distribution for halos. The comoving number density of halos with mass between M and $M + dM$ is then

$$\frac{dn}{dM} = \sqrt{\frac{2}{\pi}} \frac{\rho_M}{M} \frac{-d(\ln \sigma)}{dM} \nu_c e^{-\nu_c^2/2},$$

where $\nu_c = \delta_{\text{crit}}(z)/\sigma(M)$ is the number of standard deviations which the critical collapse density represents at mass scale M . At high mass there is an exponential cutoff above M_* , where $\sigma(M_*) = \delta_c$, and $M_* \sim 10^{13} h^{-1} M_\odot$ today. At low mass the number of halos increases rapidly.

Thus the number of halos depends on $\sigma(M)$ and $\delta_{\text{crit}}(z)$, which depend on the energy content of the Universe and the other cosmological parameters. $\sigma(M)$ is calculated based on the present mass power spectrum from observations of large scale structure in the distribution of galaxies (probing out to at least $50 h^{-1}$ Mpc), the abundance of clusters of galaxies (probing fluctuations on a scale of $8 h^{-1}$ Mpc), etc. See Eisenstein & Hu (1999, ApJ, 511, 5) for details.

At each redshift, a fixed fraction of the total dark matter mass lies in halos above the mass such that $\sigma(M) = 1$ (the 1σ mass). Thus most of the mass is in small halos at high redshift, but it continuously shifts towards higher characteristic mass at lower redshift.

Since $\sigma(M) \rightarrow \infty$ as $M \rightarrow 0$, in the CDM model, all dark matter is in halos at all redshifts provided low mass halos are included. Setting the power spectrum to 0 below a specified mass reduces the predicted number of low mass halos, and some dark matter may then not be in a halo.

At high redshifts where $\delta_{crit} \gg \sigma(M = 0)$ all halos are rare and only a small fraction of the dark matter resides in halos.

Navarro, Frenk & White (1997) worked out the mass distribution within a dark matter halo, which has a universal form.

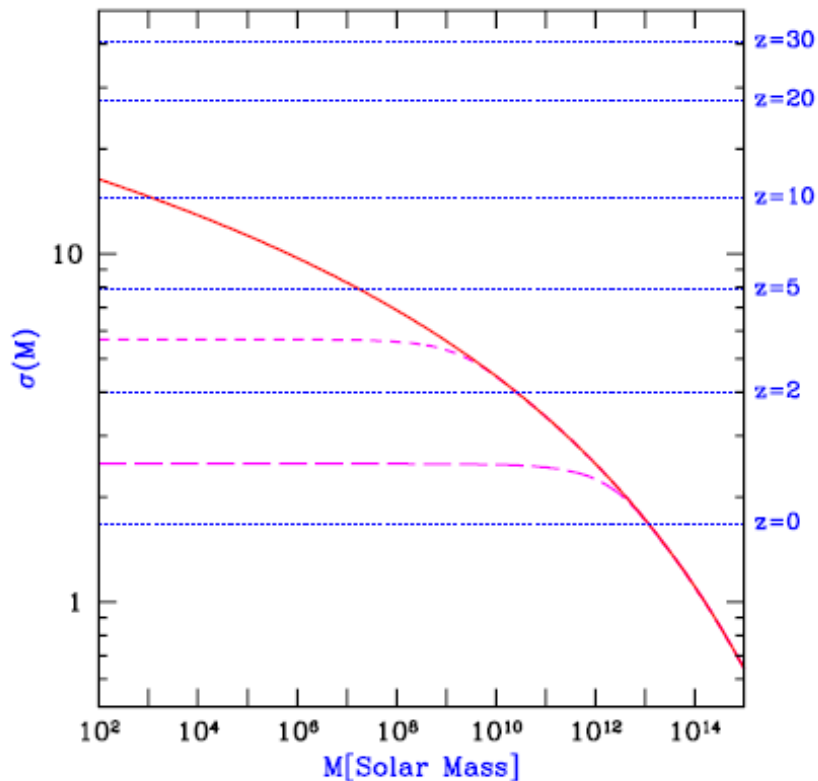


Fig. 5.— Mass fluctuations and collapse thresholds in cold dark matter models. The horizontal dotted lines show the value of the extrapolated collapse overdensity $\delta_{\text{crit}}(z)$ at the indicated redshifts. Also shown is the value of $\sigma(M)$ for the cosmological parameters given in the text (solid curve), as well as $\sigma(M)$ for a power spectrum with a cutoff below a mass $M = 1.7 \times 10^8 M_{\odot}$ (short-dashed curve), or $M = 1.7 \times 10^{11} M_{\odot}$ (long-dashed curve). The intersection of the horizontal lines with the other curves indicate, at each redshift z , the mass scale (for each model) at which a $1 - \sigma$ fluctuation is just collapsing at z (see the discussion in the text).

Fig. 9.— Fig. 5 from Barkana & Loeb, 2001.

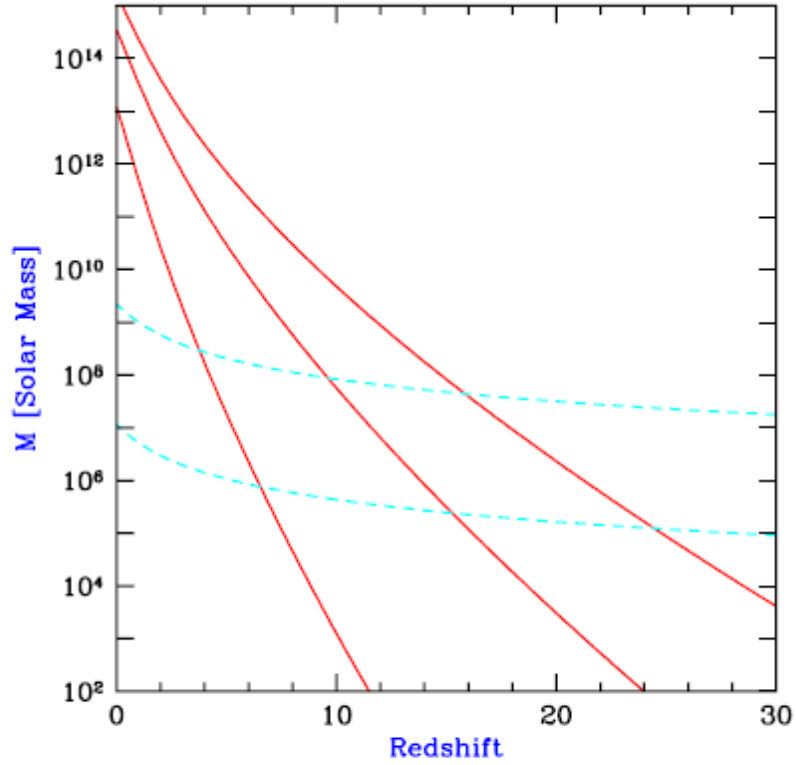


Fig. 6.— Characteristic properties of collapsing halos: Halo mass. The solid curves show the mass of collapsing halos which correspond to $1-\sigma$, $2-\sigma$, and $3-\sigma$ fluctuations (in order from bottom to top). The dashed curves show the mass corresponding to the minimum temperature required for efficient cooling with primordial atomic species only (upper curve) or with the addition of molecular hydrogen (lower curve).

Fig. 10.— Fig. 6 from Barkana & Loeb, 2001.

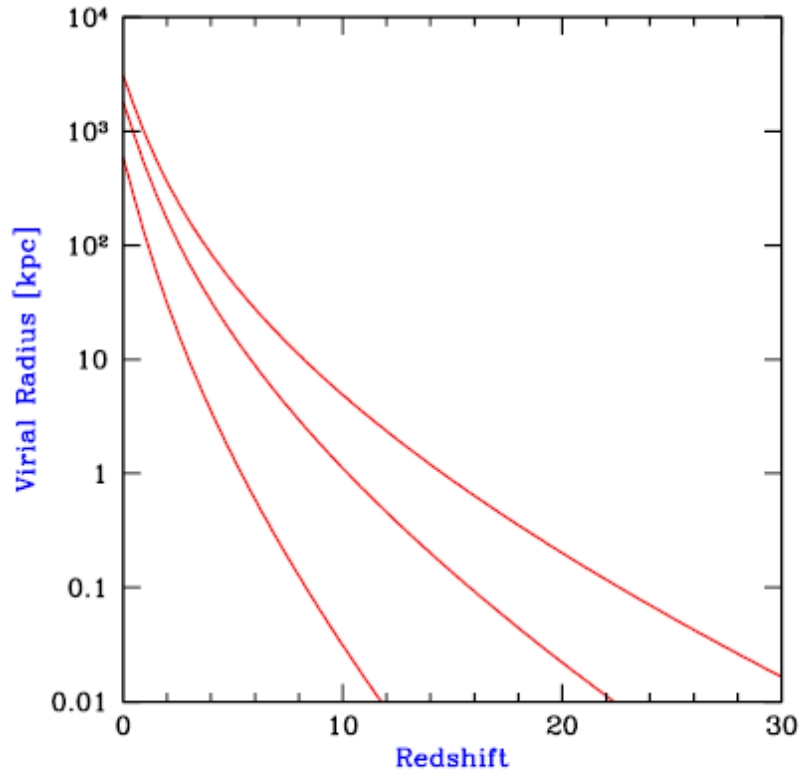


Fig. 7.— Characteristic properties of collapsing halos: Halo virial radius. The curves show the virial radius of collapsing halos which correspond to $1 - \sigma$, $2 - \sigma$, and $3 - \sigma$ fluctuations (in order from bottom to top).

Fig. 11.— Fig. 7 from Barkana & Loeb, 2001.

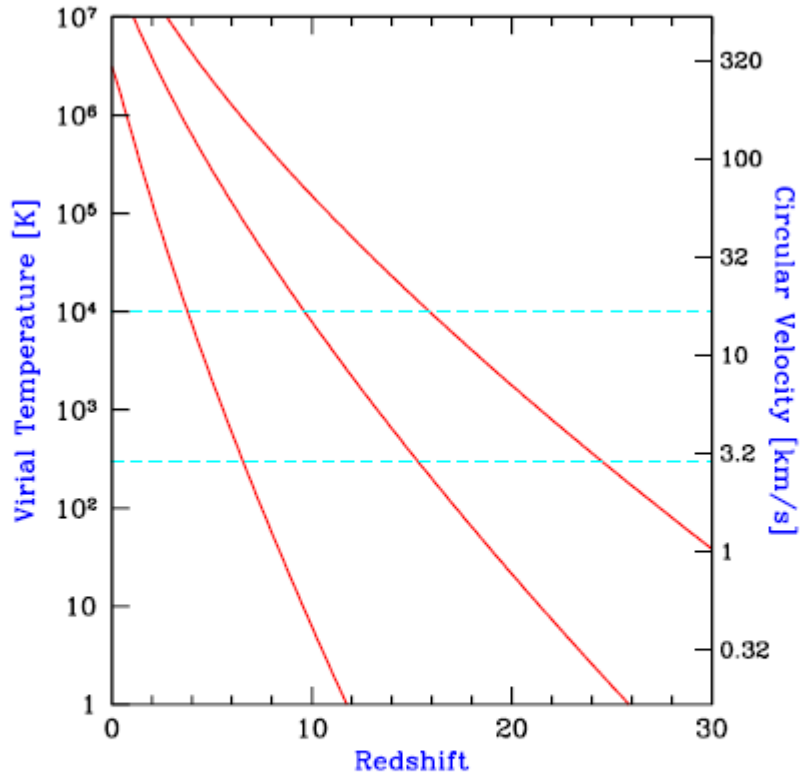


Fig. 8.— Characteristic properties of collapsing halos: Halo virial temperature and circular velocity. The solid curves show the virial temperature (or, equivalently, the circular velocity) of collapsing halos which correspond to $1 - \sigma$, $2 - \sigma$, and $3 - \sigma$ fluctuations (in order from bottom to top). The dashed curves show the minimum temperature required for efficient cooling with primordial atomic species only (upper curve) or with the addition of molecular hydrogen (lower curve).

Fig. 12.— Fig. 8 from Barkana & Loeb, 2001.

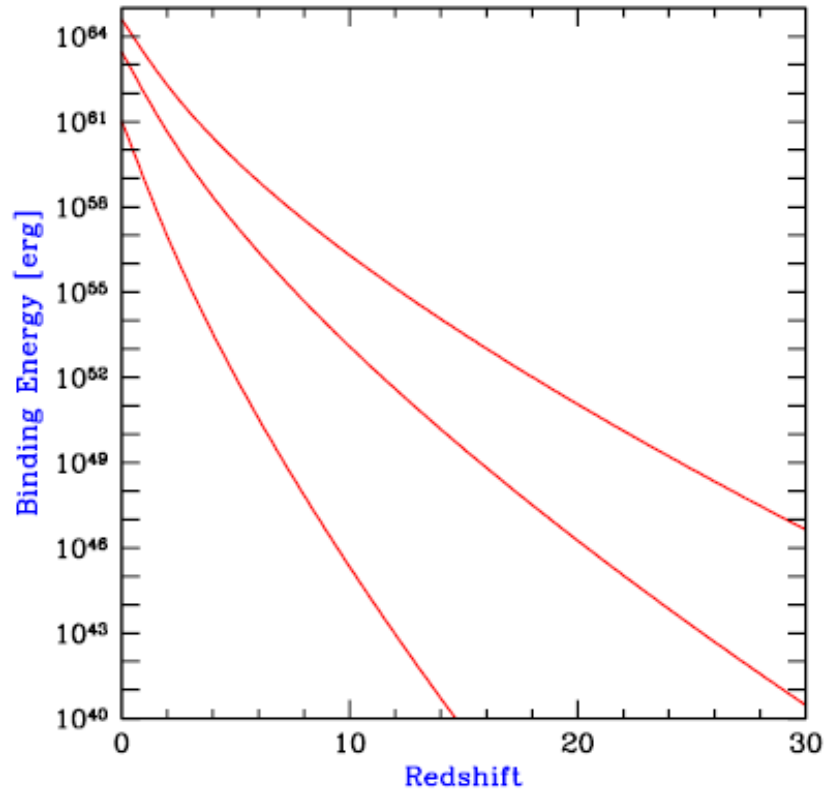


Fig. 9.— Characteristic properties of collapsing halos: Halo binding energy. The curves show the total binding energy of collapsing halos which correspond to $1 - \sigma$, $2 - \sigma$, and $3 - \sigma$ fluctuations (in order from bottom to top).

Fig. 13.— Fig. 9 from Barkana & Loeb, 2001.

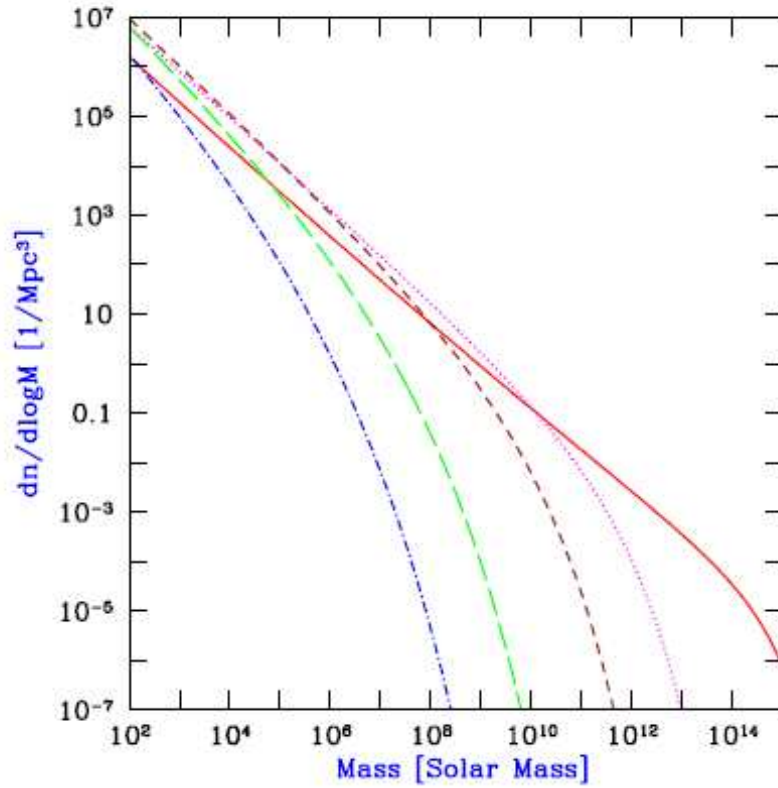


Fig. 10.— Halo mass function at several redshifts: $z = 0$ (solid curve), $z = 5$ (dotted curve), $z = 10$ (short-dashed curve), $z = 20$ (long-dashed curve), and $z = 30$ (dot-dashed curve).

Fig. 14.— Fig. 10 from Barkana & Loeb, 2001, showing the Press-Schechter halo mass function at several redshifts. At lower redshift, the most massive halos grow in mass, while the number of low mass halos declines slightly.

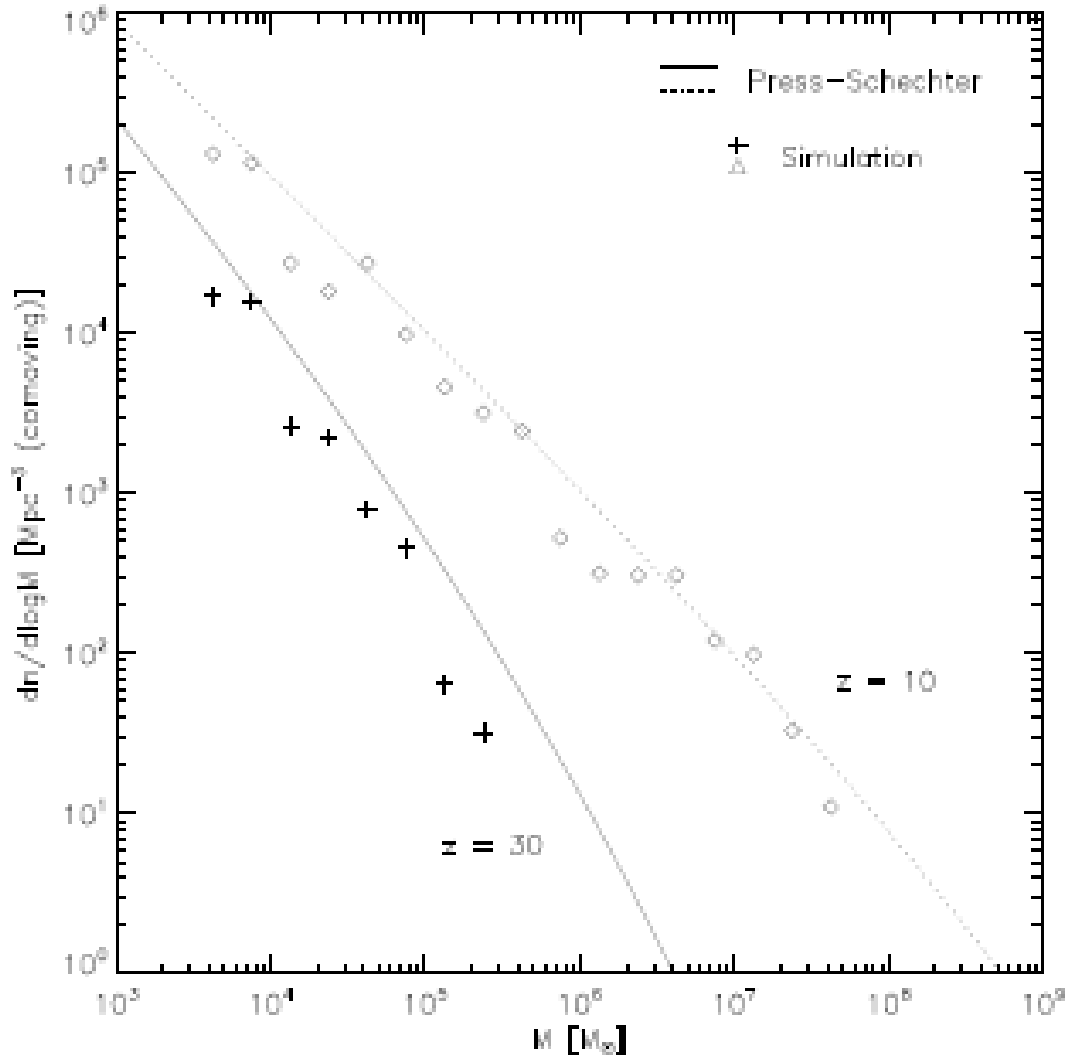


Figure 1. Comparison of the Press-Schechter mass function (solid and dotted line) and the simulation results (crosses and triangles) at $z \simeq 30$ (lower set) and $z \simeq 10$ (upper set). The simulation generally agrees with the analytic prediction, although there is a large scatter due to the finite box size. The expected number of atomic cooling haloes per cubic Mpc (comoving) at $z \simeq 10$ is of the order of 10.

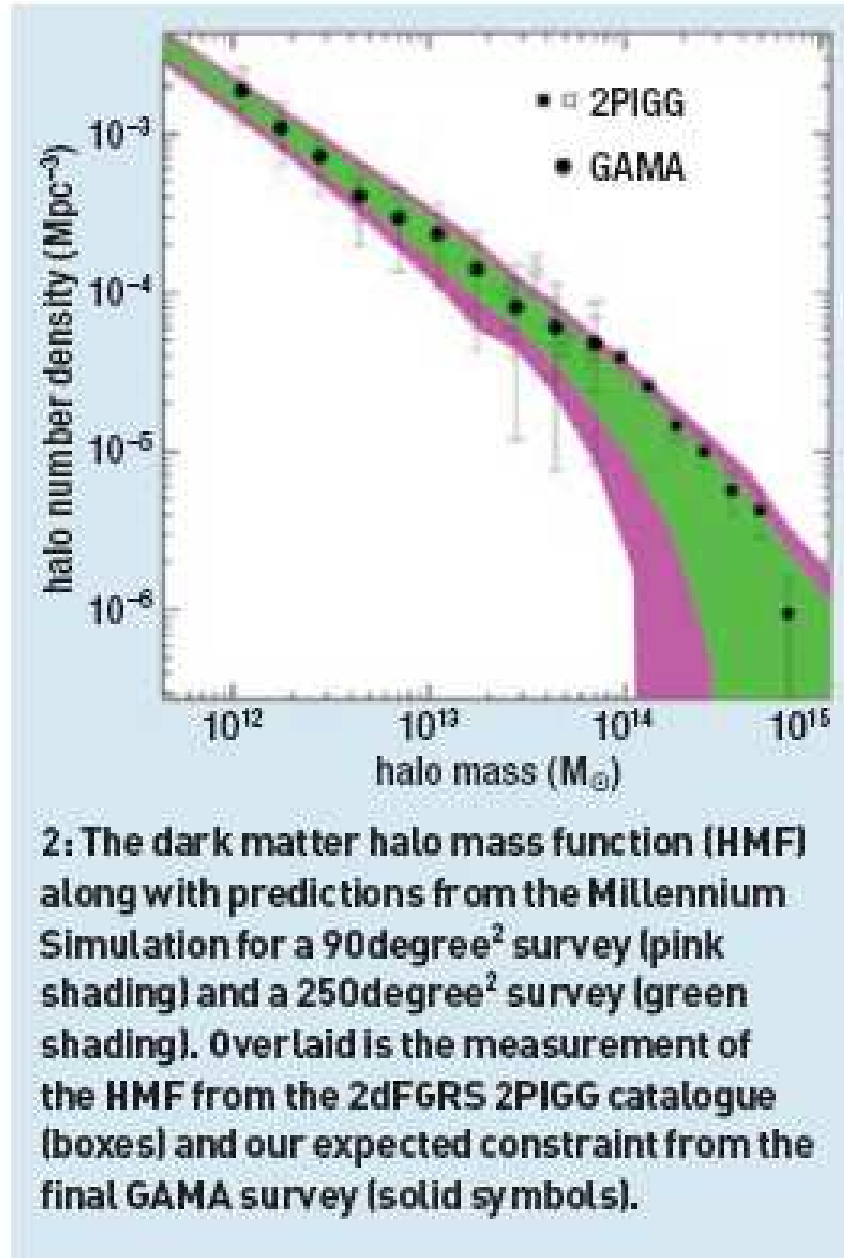


Fig. 16.— The present day halo mass function from the 2DdFGRS survey of luminous red galaxies as compared to that expected by “observing” the Millenium simulation. (Fig. from Driver, 2009, description of the GAMA project, see arXiv:0910.5123)

2. Summary

Concordance cosmology, $\Omega_m = 0.24, \Omega_b = 0.04, \Omega_\Lambda = 0.73$, flat universe with $k = 0$ and lots cold dark matter and dark energy. Predicts CMB, big bang nucleosynthesis, and the increasing recession velocity of galaxies with distance (the Hubble law).

$$z + 1 = 1/a(t)$$

Radiation dominated, becomes matter dominated at $z \sim 3500$.

Recombination at $T \sim 3000$ K, age $\sim 300,000$ yr

Perturbations established at the end of the inflation era grow in the dark matter. Perturbations are characterized by their wavelength and amplitude. At high redshift, low amplitude, low mass perturbations collapse into halos, while at low redshift these are already well developed, and high mass halos being collapsing from the larger amplitude perturbations. The details of the growth of perturbations depend on when the mode enters the horizon, whether this is before or after the universe becomes matter dominated.

The Jeans mass is that within a spherical volume of radius $\lambda_J/2$. This is the minimum mass that can collapse under the given conditions; $M_J \sim [kT/(m_p G)^{3/2} \rho^{-1/2}]$.

From $z \sim 1100$ to the time T_K for the baryons is no longer T_{CMB} , $k_J \equiv (2\pi)/\lambda = [2kT_{CMB}/3\mu m_p]^{-1/2} \sqrt{\Omega_m} H_0$, so the Jeans mass (including both baryons and dark matter) is redshift independent and has the value $M_J = 1.4 \times 10^5 M_\odot$, comparable to the mass of a globular cluster as observed today in the Milky Way halo.

At times later than z_t , the total Jeans mass becomes $\sim 5,000 M_\odot$ at $z \sim 10$.

Press & Schechter (1974) worked out an approximate number distribution of dark matter halos with mass at a redshift z for a CDM universe.

Suggested exercise:

Work out in detail the equivalent of the Saha equation for the recombination of hydrogen in a flat universe to get the fraction of hydrogen which are ionized as a function of redshift. Take into account the CMB radiation field. What assumptions do you have to make ? (Feel free to ignore helium, lithium....) Compare your results with a full numerical calculation if possible.

Suggested reading:

- a) First Light, chapter by A. Loeb and by A. Ferrara
- b) review of first stars, Bromm & Larson, 2004, ARAA, 42, 79
- c) A. Loeb, 2007, “The Frontier of Reionization: Theory and Forthcoming Observations”, Astro-ph:0711.3463
- d) R. Barkana & A. Loeb, 2001, “In the Beginning: The First Sources of Light and Reionization in the Universe”, see Astro-ph:00104683
- e) Furlanetto, Peng Oh & Briggs, 2006, Phys. Reports, 433, 181, *Cosmology at Low Frequencies: The 21 cm Transition and the High-Redshift Universe*